Supplementary Materials of the paper titled

SANE: *S*trategic *A*utonomous *N*on-Smooth *E*xploration for Multiple Optima Discovery in multi-modal and non-differentiable black-box functions

Arpan Biswas[1,a], Rama Vasudevan[2], Rohit Pant[3], Ichiro Takeuchi[3], Hiroshi Funakubo[4], Yongtao Liu[2,b]

[1] University of Tennessee-Oak Ridge Innovation Institute, Knoxville, TN 37996, USA
[2] Center for Nanophase Materials Sciences, Oak Ridge National Laboratory, Oak Ridge, TN 37830, USA
[3] Department of Materials Science and Engineering, University of Maryland, College Park, Maryland 20742, United States of America
[4] Department of Materials Science and Engineering, Tokyo Institute of Technology, Yokohama, 226-8502, Japan

Appendix A. Additional Formulation

1. *Branin Function:*

$$f(X) = a\left(x_2 - bx_1^2 + cx_1 - r^2\right) + s(1-t)\cos\left(x_1\right) + s \tag{S1}$$

Where,

$$a = 1; b = \frac{5.1}{4\pi^2}; c = \frac{5}{\pi}; r = 6; s = 10; t = \frac{1}{8\pi};\ -5 \le x_1, x_2 < 15$$

2. *Gaussian Process (GP) Regression:*

The general form of the GPM is as follows:

$$y(x) = x^T\beta + z(x) \tag{S2}$$

where $x^T\beta$ is the Polynomial Regression model. The polynomial regression model captures the global trend of the data. $z(x)$ is a realization of a correlated Gaussian Process with mean $E[z(x)]$ and covariance $cov(x^i, x^j)$ functions defined as follows:

$$z(x) \sim GP\left(E[z(x)], cov\left(x^i, x^j\right)\right); \tag{S3}$$

$$E[z(x)] = 0,\ cov\left(x^i, x^j\right) = \sigma^2 R\left(x^i, x^j\right) \tag{S4}$$

$$R\left(x^i, x^j\right) = \exp\left(-0.5 * \sum_{m=1}^{d} \frac{\left(x_m^i - x_m^j\right)^2}{\theta_m^2}\right); \tag{S5}$$

$$R(x^i,x^j) = \exp\left(-\sqrt{5}\times\sum_{m=1}^{d}\frac{|x_m^i - x_m^j|}{\theta_m}\right)\times\left(1+\sqrt{5}\times\sum_{m=1}^{d}\frac{|x_m^i - x_m^j|}{\theta_m}+\frac{5}{3}\times\sum_{m=1}^{d}\frac{\left|x_m^i - x_m^j\right|^2}{\theta_m^2}\right) \tag{S6}$$

$$\theta_m = (\theta_1,\theta_2,....,\theta_d)$$

where σ^2 is the overall variance parameter and $\theta_m$is the correlation length scale parameter in dimension *m* of *d* dimension of x. These are termed as the hyper-parameters of GP model. $R(x^i,x^j)$ is the spatial correlation function. In this paper, we have considered a Radial Basis function which is given by eqn. S5 and Matern kernel function as per eqn. S6. The objective is to estimate the hyper-parameters $\sigma,\ \theta_m$ which creates the surrogate model that best explains the training data D_k at iteration *k*. In this paper, we used the Monte Carlo Markov Chain (MCMC) approach to estimate the hyperparameters.

After the GP model is fitted, the next task of the GP model is to predict at an arbitrary (unexplored) location drawn from the parameter space. Assume $D_k = \{X_k, Y(X_k)\}$ is the prior information from previous evaluations or experiments from high fidelity models, and $\bar{\bar{x}}_{k+1} \in \bar{\bar{X}}$ is a new design within the unexplored locations in the parameter space, $\bar{\bar{X}}$. The predictive output distribution of x_{k+1}, given the posterior GP model, is given by eqn S7.

$$P\left(\bar{y}_{k+1}\middle|D_k,\bar{\bar{x}}_{k+1},\sigma_k^2,\theta_k\right) = N\left(\mu\left(\bar{y}_{k+1}\left(\bar{\bar{x}}_{k+1}\right)\right),\sigma^2\left(\bar{y}_{k+1}\left(\bar{\bar{x}}_{k+1}\right)\right)\right) \tag{S7}$$

where:

$$\mu\left(\bar{y}_{k+1}\left(\bar{\bar{x}}_{k+1}\right)\right) = cov_{k+1}^{\ T}COV_k^{-1}Y_k; \tag{S8}$$

$$\sigma^2\left(\bar{y}_{k+1}\left(\bar{\bar{x}}_{k+1}\right)\right) = cov\left(\bar{\bar{x}}_{k+1},\bar{\bar{x}}_{k+1}\right) - cov_{k+1}^{\ T}COV_k^{-1}cov_{k+1} \tag{S9}$$

COV_k is the kernel matrix of already sampled designs X_k and cov_{k+1} is the covariance function of new design $\bar{\bar{x}}_{k+1}$ which is defined as follows:

$$COV_k = \begin{bmatrix} cov(x_1,x_1) & \cdots & cov(x_1,x_k) \\ \vdots & \ddots & \vdots \\ cov(x_k,x_1) & \cdots & cov(x_k,x_k) \end{bmatrix}$$

$$cov_{k+1} = [cov(\bar{x}_{k+1}, x_1), cov(\bar{x}_{k+1}, x_2), .., cov(\bar{x}_{k+1}, x_k)]$$

3. *Expected Improvement acquisition function:*

$$EI(\bar{y}(\bar{x} \mid f = 1)) =$$

$$\begin{cases} (\mu(\bar{y}(\bar{x})) - y(x^+) - \xi) \times \Phi(Z,0,1) + \sigma(\bar{y}(\bar{x})) \times \phi(Z) & if\ \sigma(\bar{y}(\bar{x})) > 0 \\ 0\ if\ \sigma(\bar{y}(\bar{x})) = 0 \end{cases} \quad \text{(S10)}$$

$$Z = \begin{cases} \dfrac{\mu(\bar{y}(\bar{x})) - y(x^+) - \xi}{\sigma(\bar{y}(\bar{x}))} & if\ \sigma(\bar{y}(\bar{x})) > 0 \\ 0 \ \ if \sigma(\bar{y}(\bar{x})) = 0 \end{cases} \quad \text{(S11)}$$

where $y(x^+)$is the current maximum value among all the sampled data until the current stage ; $\mu(\bar{y})$ and $\sigma(\bar{y})$ are the predicted mean and standard deviation from GP; $\Phi(.)$ is the cdf; $\phi(.)$ is the pdf; $\xi \geq 0$ is a small value which is set as 0.01.

Appendix B. Additional Figures

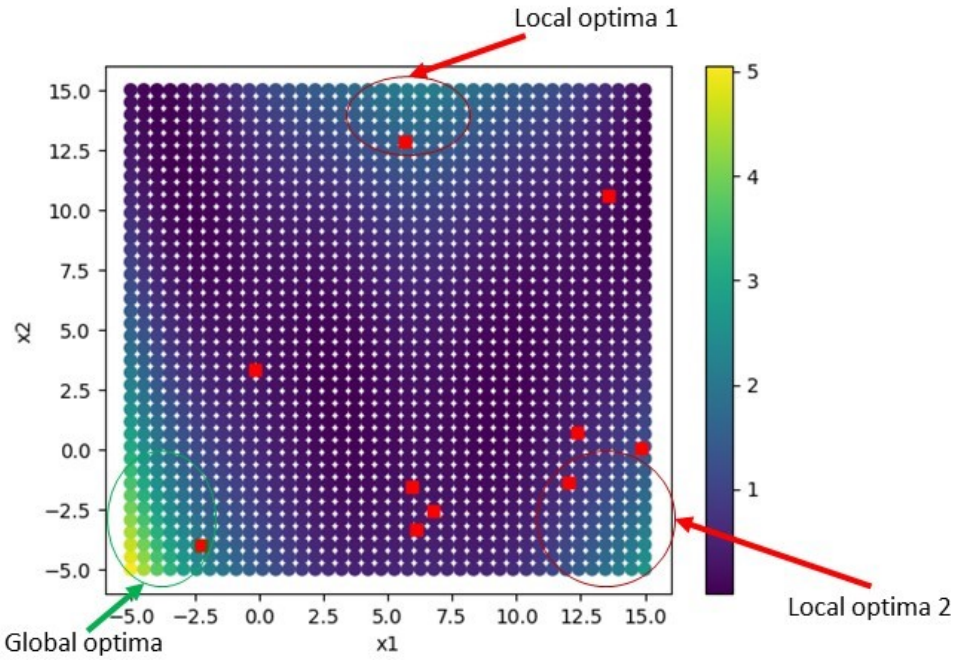

Figure S1. Second initialization with 10 starting samples randomly selected (denoted by red dots). Here, at least one sample is located very near to the optimal regions.

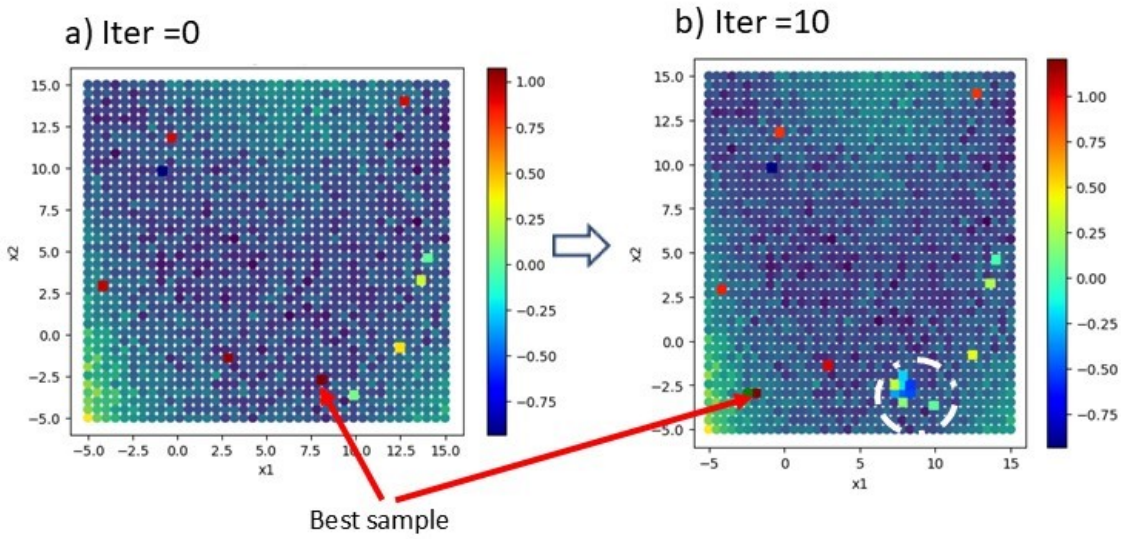

Figure S2. Additional plots of Fig 4c. where ground truth is added with noise scale of 50%, randomly generated from normal distribution. Here, during the initialization, due to extreme noise, a fake optima location is generated (fig. a), with the best location marked with arrow. Then for the next 10 iterations, SANE gained knowledge to move towards the true optima as marked with arrow in fig. b.

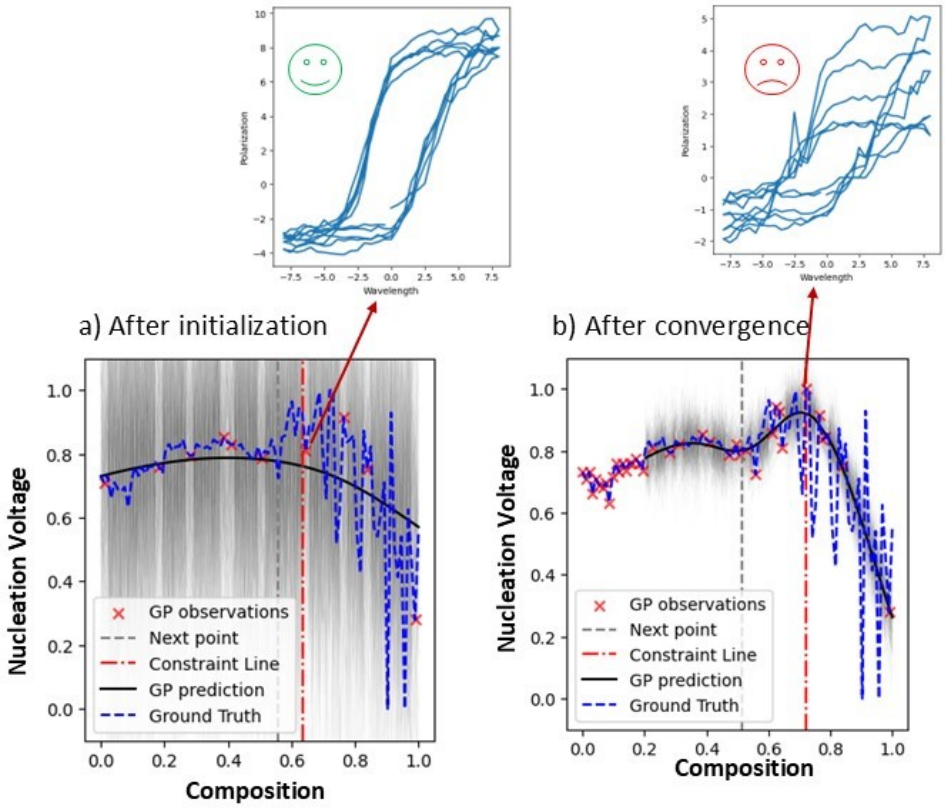

Figure S3. Figs (a), (b) show an example of the prediction of the constraint line after initialization and after SANE convergence respectively. We can see after prediction from early assessment the good sample is in the infeasible region and with more collection of samples the predicted constraint boundary can be tuned better.

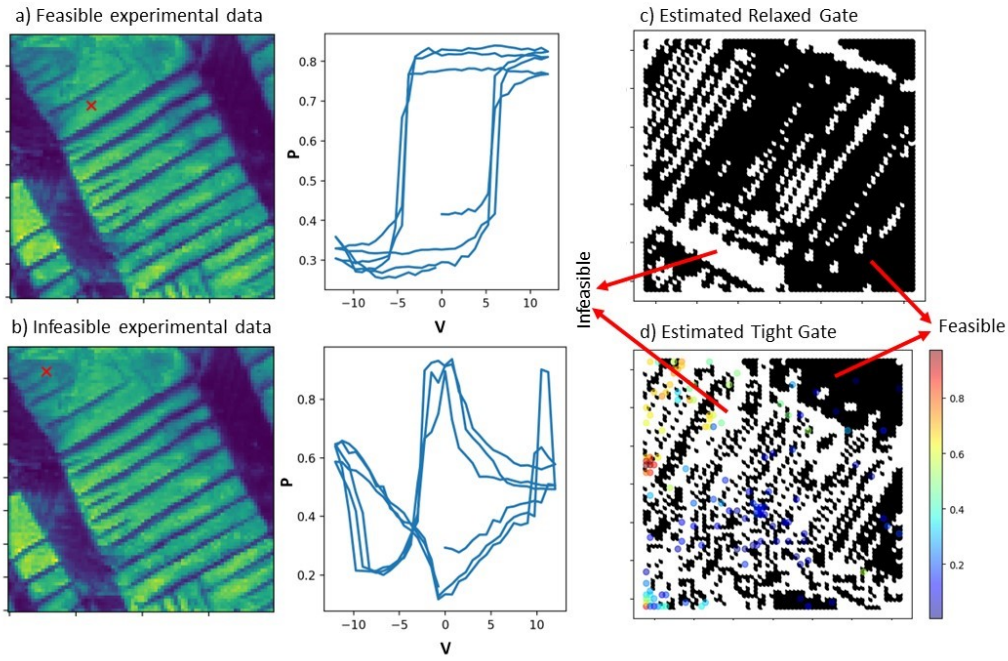

Figure S4. Figs (a),(b) show an example of the spectral with positive and negative assessment respectively. These two samples are among the initial 30 samples generated from LHS approach. Fig (c) shows the map of the relaxed gate estimated from the initial data only. Fig (d) shows the map of the tight gate estimated after the exploration cost is exhausted. It is to be noted here that the gate is tightened dynamically as the SANE exploration continues, however, without human intervention. The human assessment is only done for the initial 30 samples. We can see there are some samples selected but located in the estimated infeasible region, those were the part of the feasible region during the respective stages of the iterations. Thus, tightening the constraint also seems to gradually avoid over exploration of a certain region too. However, it can induce the SANE to miss a region of interest (refer to Fig. 6c,d), particularly in the later stage of exploration. Therefore, tuning the penalty factor, P is another alternative to relax the gate.

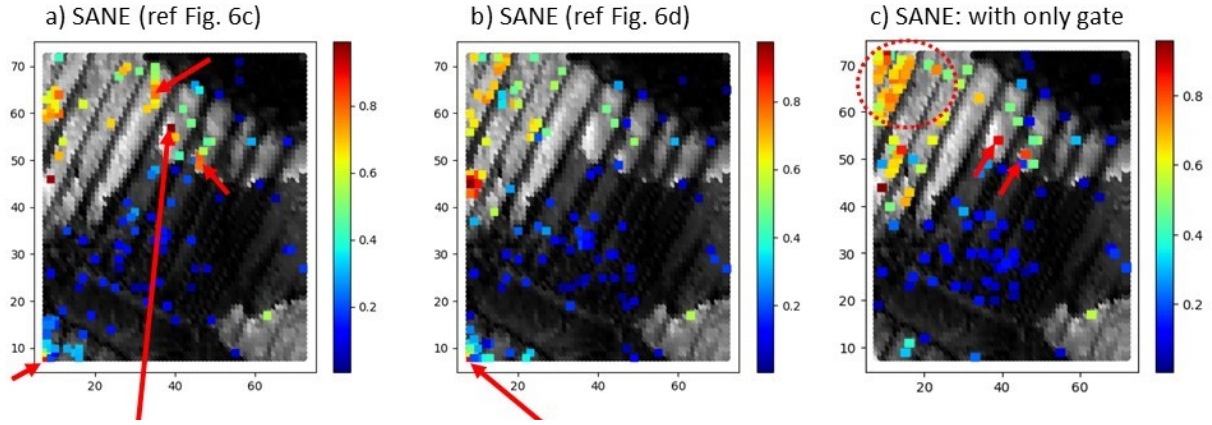

Figure S5. Additional comparison of different SANE exploration in BEPS data of a PbTiO3 (PTO) thin film, Fig(a) is the SANE exploration with relaxed human-intervened gate (ref# fig 6c in main text), fig(b) is the SANE exploration with hard human-intervened gate (ref# fig 6c in main text), fig(c) is the SANE exploration with standard Expected Improvement acquisition function and integration of gate. The color of the explored points indicates the loop area value where red indicates the higher values (optimal regions) and blue indicates the lower values. We can see the gate also plays a role in better exploration and it is able to locate some good regions (marked with arrows in fig c.). However, with standard acquisition function, it fails to exploit, once those regions are discovered, unlike in fig. a. Thus, we can see in fig. a, with more exploitation, better and more good local solutions are found (marked with arrows in fig. a.). Additionally, the standard acquisition function is overly concentrated in one area (marked with circle in fig. c). Therefore, it fails to discover another local area of interest which all the SANE with hybrid acquisition function able to discover (bottom left corner of the images in fig. a, b as marked with arrows).